Electronic Supplementary Material (ESI) for Physical Chemistry Chemical Physics.

Supporting Information

Determining the role of redox-active materials during laser-induced water decomposition

Mark-Robert Kalus[a], Riskyanti Lanyumba[a], Nerea Lorenzo-Parodi[b], Maik A. Jochmann[b], Klaus Kerpen[b], U. Hagemann[c], Torsten C. Schmidt[b], Stephan Barcikowski[a*], and Bilal Gökce[a]

[a]Technical Chemistry I, University of Duisburg-Essen and Center for Nanointegration Duisburg-Essen (CENIDE), Universitaetsstrasse 7, 45141 Essen, Germany

[b]Instrumental Analytical Chemistry and Centre for Water and Environmental Research (ZWU), Universitaetsstrasse 5, 45141 Essen, Germany.

[c]Interdisciplinary Center for Analytics on the Nanoscale (ICAN) and Center for Nanointegration Duisburg-Essen (CENIDE), University of Duisburg-Essen, Carl-Benz-Strasse 199, 47057 Duisburg, Germany

This supporting information provide additional information on the solvent decomposition process and the oxidation behavior of the nanoparticles during laser ablation of a gold, platinum, silver, copper and titanium bulk target in water.

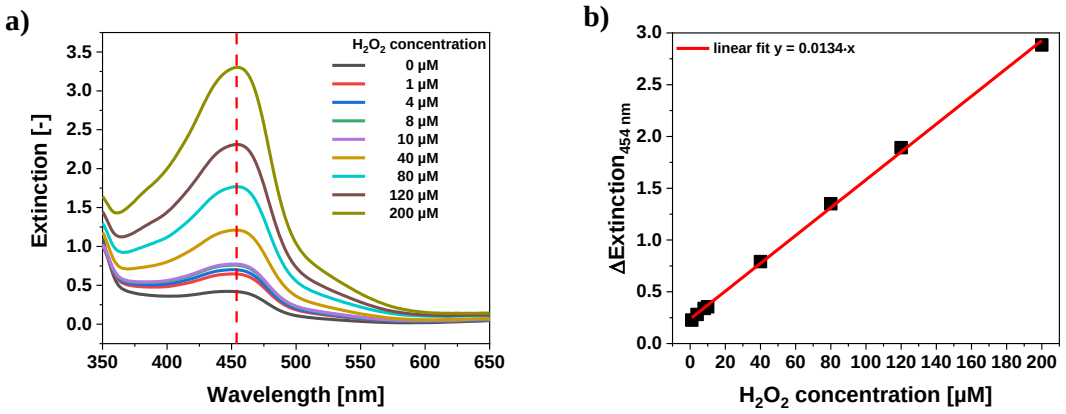

Fig. S1: (a) Absorption spectrum of the DMP-solutions treated with H_2O_2 concentrations of 0-200 uM. (b) Calibration plots for the determination of H_2O_2 concentration.

Fig. S1a summarizes the UV/Vis spectra of the DMP-solutions treated with different hydrogen peroxide concentrations (0-200 µM). The extinction values at a wavelength of 454 nm were extracted from the UV/vis spectra and subtracted from the blank. By plotting the results against the added hydrogen peroxide concentration, a calibration plot is derived as illustrated in Fig. S2b.

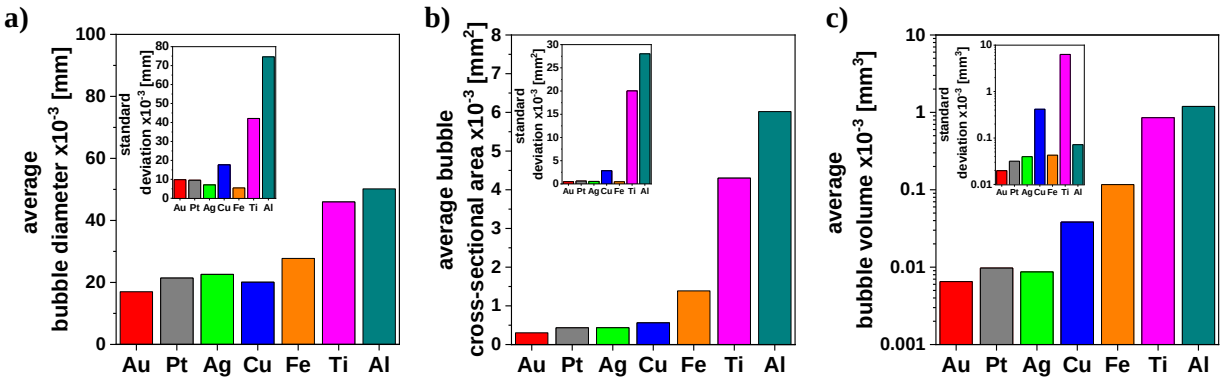

Fig. S2: Average bubble diameter (a), cross-sectional area (b) and bubble volume for persistent microbubbles produced during LAL of gold, platinum, silver, copper, iron, titanium and aluminum in water.

Fig. S2 summarizes the individual properties such as the average bubble diameter (Fig. S2a), average bubble cross-sectional area (Fig. S2b) and the average bubble volume for persistent microbubbles produced during laser ablation of gold, silver, copper, iron, titanium and aluminum in water.

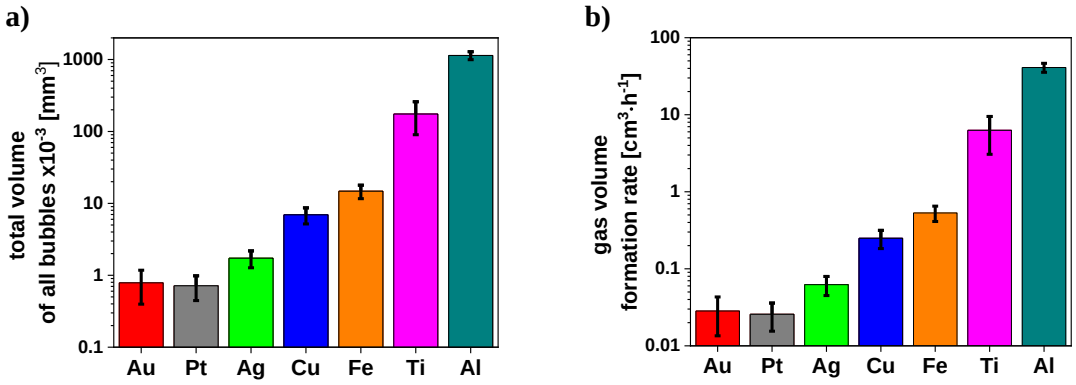

Fig. S3: Total volume of all persistent microbubbles recorded (a) and the corresponding gas volume formation rate basing on the recording time (b).

In Fig. S3a the total volume of all persistent microbubbles per image was calculated.

Considering the recording time for every image, the gas volume formation was determined as shown in Fig. S3b.

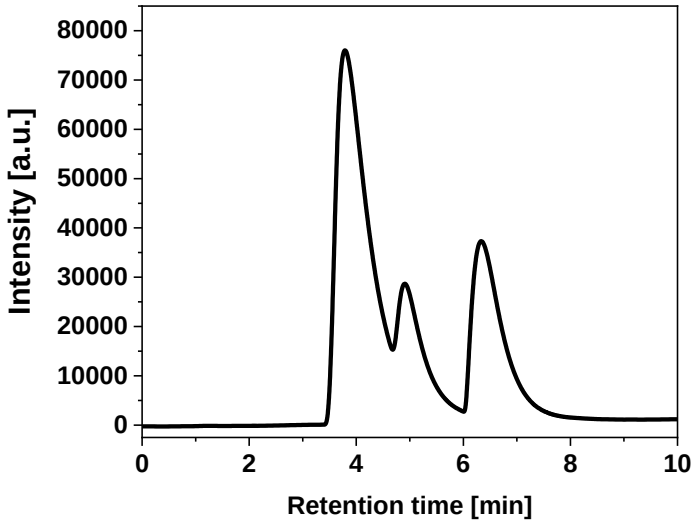

Fig. S4: Exemplary raw gas chromatogram of gases produced during LAL of platinum in water.

Fig. S4 demonstrates an exemplary raw gas chromatogram showing the composition of gases produced after LAL of platinum in water. Analogous raw gas chromatograms with different peak intensities were obtained for LAL of gold, silver, copper, iron, titanium and aluminum in water. For all the gas chromatograms baseline correction was performed followed by computational deconvolution and subsequent fitting of the single peaks with a Gaussian function.

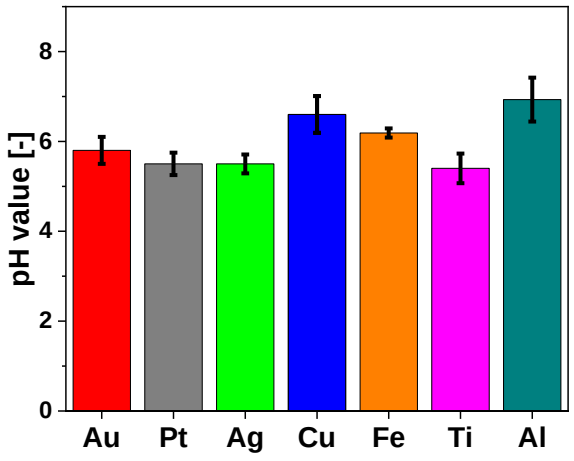

Fig. S5: Measured pH values of the colloids after laser ablation.

Fig. S5 shows the pH values measured for the gold, platinum, silver, copper, iron, titanium and aluminum colloids directly after LAL. No specific material dependent trend is visible.

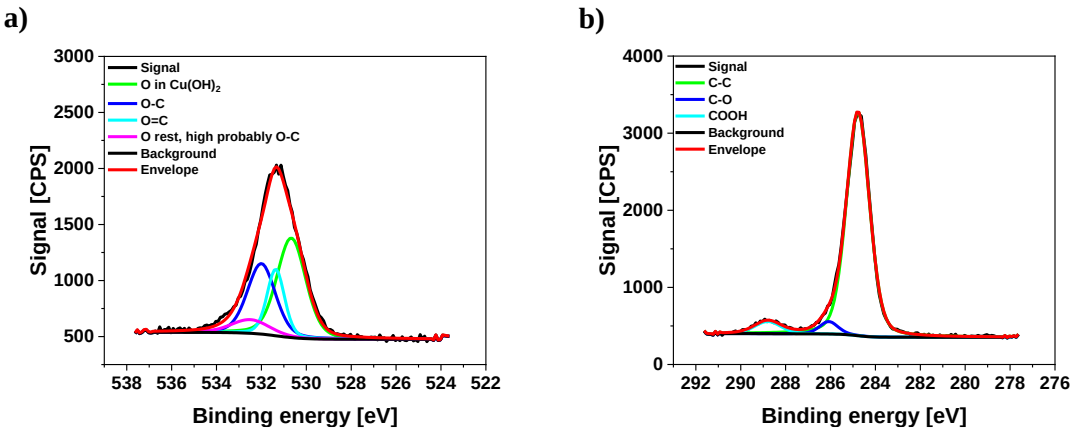

Fig. S6: XPS oxygen (a) and carbon (b) peak of Cu NPs produced by laser ablation in water.

The XPS measurements of Cu NPs produced by LAL in water gave hints that only elemental copper and copper hydroxide ($Cu(OH)_2$) species are present These can be justified as follows: First, the shake-ups in the Cu2p signal around 940 eV are very similar to those expected for the hydroxides or CuO [88]. However, regarding the peak shape there is a tendency for hydroxides (left flank at 945 eV is stronger than the right flank at 940 eV). This is supported by the oxygen binding energy of CuO which is typically located at 530 eV or below [88]. In contrast, the oxygen binding energy in the hydroxides is typically located at 531 eV [88] and thus more corresponding to the measured values (see Fig. S6a). Second, the oxygen intensity (taking into account the carbon-oxygen intensities) corresponds to a ratio of Cu to O of 1 to 2 indicating the presence of hydroxides instead of CuO. Third, from literature it is known that Cu_2O shows barely visible shake-ups [88]. Concluding, Cu_2O cannot be responsible for the intensities greater than 933eV in Cu2p. The Cu2p intensity at 932eV is then either elemental Cu or Cu_2O. However, a small unidentified amount of oxygen remains, which would correspond well to the Cu intensity at 932 eV and a ratio of 2 to 1 for Cu to O. The missing fit intensity for the oxygen fit at binding energies of 533-534 eV is then likely attributed to the formation of carbon-containing O bonds attached to the NP surface, which are within the error of the carbon signal (see Fig. S6b).

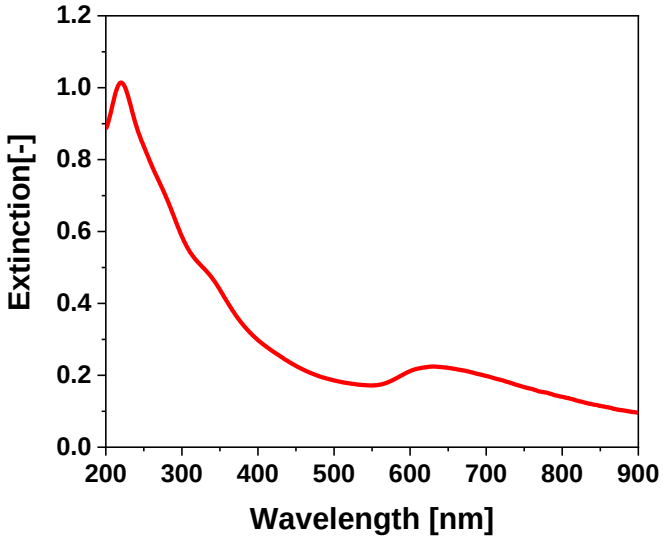

Fig. S7: UV-Vis spectrum of copper colloids produced at a laser fluence of 283 J/cm^2 and a liquid-flow of 300 ml/min.

Fig. S7 displays the UV-Vis spectrum of laser-generated copper colloids in water. Here, the peaks at around 200 nm, 330 nm and 600 up to 700 nm can be attributed to the presence of oxidic copper nanoparticles.